의학석사 학위논문

# 선행화학요법을 시행 받는 유방암 환자에서 병리학적 완전 관해를 예측하는 데에 있어서 확산강조 자기공명영상에서 겉보기확산계수의 변화의 역할

# Change in the ADC Value on Diffusion-Weighted MRI as a Predictive Tool for Pathologic Complete Response in Patients with Breast Cancer Undergoing Neoadjuvant Chemotherapy

울 산 대 학 교 대 학 원

의 학 과

박 아 름

# 선행화학요법을 시행 받는 유방암 환자에서 병리학적 완전 관해를 예측하는 데에 있어서 확산강조 자기공명영상에서 겉보기확산계수의 변화의 역할

지도교수 김 학 희

이 논문을 의학석사학위 논문으로 제출함

2022 년 2 월

울 산 대 학 교 대 학 원
의 학 과
박 아 름

박아름의 의학석사학위 논문을 인준함

심사위원 차 주 희 인
심사위원 김 학 희 인
심사위원 채 은 영 인

울 산 대 학 교 대 학 원
2022 년 2 월

# 감사의 글

영상의학과 전공의 수련을 마친 후 유방 파트를 선택하고 서울아산병원 유방 파트에서 2년간 전임의를 하게 된 것은 제 인생에서 새로운 페이지를 쓰게 된 것과 같습니다. 신입 유방 전문의로서 부족한 것이 많았던 제가 지식과 경험을 쌓아 나가면서 흥미와 자부심을 갖게 되고, 이렇게 석사과정을 기쁘게 마칠 수 있도록 이끌어 주신 김학희 지도 교수님께 깊은 감사를 드립니다. 전임의 생활을 하고 석사를 수료하는 지난 3년동안 교수님으로부터 지식 뿐만 아니라 의사로서 가지는 자세와 마음에 대해서도 배울 수 있었습니다. 여기서 배우고 경험한 것들이 저의 향후 인생에 밑거름이 될 것입니다. 그리고 유방 파트의 책임자로서 항상 든든하게 지켜봐 주시고 즐겁게 가르침을 주신 심사위원장 차주희 교수님께도 감사드립니다. 또한, 논문 작성에서 느껴지는 어려움들을 깨고 나아가는 데 도움을 주시고 조언을 해주신 심사위원 채은영 교수님께도 감사의 말씀을 올립니다. 아울러, 석사를 시작하는 전임의 생활을 하는 동안 지식과 경험을 늘려 주시고 조언과 지원을 아끼지 않으신 신희정 교수님, 최우정 교수님께도 감사드립니다.

전임의 2년을 마친 후 서울대학교 병원에 가서 석사 과정의 마지막 두 학기를 이어나갔습니다. 새로운 환경이었지만 잘 적응하게 해 주시고 지식과 연구의 열정을 보여주시며 가르쳐 주신 문우경 교수님, 조나리야 교수님, 장정민 교수님께 감사드립니다. 1년동안 많은 것을 배우고 경험하게 해 주셨습니다.

이 자리에 있기까지 저를 키워주신 어머니, 아버지께 감사드립니다. 부모님의 사랑과 열정적 지원 없이는 지금의 제가 존재할 수 없었을 것입니다. 또한 든든한 지원군이 되어주신 시어머니, 시아버님께도 감사의 말씀을 올립니다.

저를 옆에서 한결같이 사랑해주고 든든한 버팀목이 되어준 남편 서인호, 고맙고 사랑합니다. 남편이 있었기에 이 모든 과정들을 자신 있게 시작하고 기쁘게 마칠 수 있었습니다. 그리고 언젠가 이 글을 읽게 될 출생 후 백일이 되고 넘치는 기쁨과 사랑을 알게 해 준 아들 서주호 사랑합니다.

## 초 록

Diffusion-weighted imaging (DWI)에서 측정되는 겉보기확산계수 (apparent diffusion coefficient, 이하 ADC)는 선행화학요법 (neoadjuvant chemotherapy, 이하 NAC)을 시행 받는 유방암 환자에서 종양의 병리학적 반응을 예측하는 데에 이용될 수 있다. 종양의 NAC에 대한 반응은 유방암의 분자학적 아형에 따라서 다르다. 하지만 병리학적 완전 관해 (pathological complete response, 이하 pCR)의 예측 인자로서 사용되는 ADC 값의 유용성에 대해서 종양 분자 아형의 효과를 고려하여 분석한 연구는 부족하다. 따라서, 본 연구는 NAC를 시행 받는 유방암 환자에서 NAC 종료 후 pCR 획득을 예측하는 데에 사용될 수 있는 ADC의 효과에 대해서 ADC 값과 종양의 아형 사이의 상호작용 효과를 포함하여 분석하고자 하였다.

2015년도에서 2018년도 사이에 NAC 전후로 유방 자기공명영상 (magnetic resonance imaging, 이하 MRI)을 시행 받고 이후에 수술을 시행 받은 유방암 여성 환자들을 후향적으로 확인하여 포함하였다. NAC 전과 후 종양의 평균 ADC 값 (이하 각각 $ADC_{pre}$ and $ADC_{post}$)을 측정하였고 종양의 평균 ADC 값의 변화 (ΔADC)를 다음과 같이 계산하였다. $\Delta ADC = ADC_{post} - ADC_{pre}$. 종양의 병리학적 반응은 Miller & Payne grading system에 따라서 완전 관해 (pCR) 혹은 불완전 관해 (non-pCR)의 두 가지로 분류하였다.

이 연구에 최종적으로 포함된 434명의 여성 중 103명 (23.7%)이 pCR을 획득하였고 (pCR 군), 331명 (76.3%)가 pCR을 획득하지 못하였다 (non-pCR 군). $ADC_{post}$와 ΔADC 값들이 pCR 군과 non-pCR 군 사이에 유의한 차이를 보였다 (각각 1.5±0.5 vs. 1.2±0.4 및 0.5±0.6 vs. 0.2±0.4; $P<0.001$). 전체 환자군에서 pCR을 예측하는 데에 있어서 종양의 아형과 ΔADC 사이에 유의한 상호작용 효과가 관찰되었다 ($P$ for interaction=0.02). 종양의 아형들 중에서는 오직 HER2-enriched 아형에서만 ΔADC가 pCR과 유의한 연관성을 보였다 (adjusted odds ratio= 5.70, $P=0.04$). 수신자 조작 특성곡선 (receiver operating characteristic (ROC) curve 분석에서는, 곡선하면적 (area under the curve, 이하 AUC)이 전체 환자군에서 0.65, 또한 HER2-enriched 아형에서 0.77로 관찰되었다.

결론적으로, 이 연구의 결과는 유방암 환자에서 NAC 종료 후 DWI에서 종양의 평균 ADC 값의 증가는 pCR을 예측하는데 이용될 수 있다는 점을 시사한다. 또한 이러한 ADC 값의 변화는 HER2-enriched 아형에서만 pCR의 독립적인 예측인자로 작용하였다.

# Contents

## List of Tables



## List of Figures

# 1. Introduction

## 1.1 Research background

Neoadjuvant chemotherapy (NAC) is increasingly used for patients with proven lymph node metastasis and to reduce the tumor volume . Studies have shown that NAC is as effective as adjuvant chemotherapy in terms of locoregional control and survival outcomes. Furthermore, pathologic complete response (pCR) after NAC has been demonstrated to be a surrogate endpoint for prediction of a long-term survival benefit ; therefore, there have been many efforts to predict pCR with imaging studies for presurgical planning.

Diffusion-weighted imaging (DWI) is a functional imaging technique that depicts the diffusivity of water molecules in tissues, and the degree of water diffusion in a tissue is inversely correlated with the tissue cellularity and the integrity of cell membranes . The apparent diffusion coefficient (ADC) value is a quantitative measurement of diffusion calculated on DWI performed at different *b* values. Cytotoxic effects associated with chemotherapy induce changes in the biological environment in the damaged tissue, leading to less restrictive conditions for water diffusion and thereby to an increase in the tumor ADC value. Contrast-enhanced MRI is frequently used and known be able to accurately evaluate the tumor response to NAC . However, it has some limitations compared with DW MRI, such as a longer duration time, requirement for contrast agents, and difficulty in differentiating viable residual tumor from scar tissue after NAC. Previous studies have demonstrated the tumor ADC as a potential imaging biomarker to predict the pathological tumor response. Park et al studied the potential of pretreatment ADC values, and Liu et al studied the efficacy of DWI with pre- and post-NAC ADC values to predict pCR. The American College of Radiology Imaging Network (ACRIN) 6698 multicenter–study revealed that the change in the tumor ADC midtreatment and posttreatment was similarly predictive of pCR .

The response to NAC varies according to the molecular subtype of breast cancer, and approximately 6% to 45% of patients are reported to achieve pCR . However, only a few studies have demonstrated the usefulness of the ADC as a predictor of pCR while considering the effect of the tumor subtype.

## 1.2 Research proposal

Therefore, the purpose of this study was to evaluate the impact of the change in the tumor ADC value (ΔADC) after completion of treatment to predict pCR in patients with breast cancer undergoing NAC and to assess the predictive value of ΔADC with relation to tumor subtype using an interaction effect analysis.

## 2. Materials and Methods

### 2.1. Patients

This retrospective study from a single tertiary center was approved by the institutional review board, and the requirement to obtain informed consent was waived. Women with breast cancer who received NAC from January 2015 to December 2018 were included. We identified consecutive women with breast cancer who underwent MRI before and after NAC (MRI1 and MRI2, respectively) and subsequent surgery. Exclusion criteria included women who had vacuum-assisted or excisional biopsy before the pretreatment MRI, either pretreatment or posttreatment MRI performed at an outside institution or missing, MRI insufficient for analysis, or incomplete patient data. Patients received standard NAC treatment according to the tumor subtypes. NAC regimens were mainly anthracycline-based and/or anthracycline/taxane based. Patients with human epidermal growth factor 2 (HER2)-positive cancer also received trastuzumab.

### 2.2. MRI acquisition

Breast MRI was performed using either a 1.5-T or 3.0-T MRI scanners (Avanto or Skyra, Siemens Medical Solutions; Ingenia, Philips Medical Systems) with a dedicated 18-channel breast coil in the prone position. The MRI protocols were as follows: an axial T2-weighted sequence and an axial fat-suppressed dynamic T1-weighted sequence of one unenhanced and five DCE acquisitions with a temporal resolution of 61 sec. An intravenous bolus injection of 0.1 mmol/kg of gadoterate meglumine (Uniray, Dongkook Pharmaceutical) was administered at a flow rate of 2 mL/sec followed by a 20-mL saline flush. Before the dynamic series, DWI was performed according to the following protocols. At 1.5-T, a single-shot echo-planar imaging (ss-EPI) sequence was performed with the following parameters: repetition time/echo time (TR/TE), 10200/67 ms; field-of-view (FOV), 340×204 mm; acquisition matrix, 256×160; slice thickness, 3 mm; acquisition time, 6:46; spatial resolution, 1.4×1.4×3.0 mm; and b-values of 0, 800, and 1200 sec/mm$^2$ on a Siemens Magnetom Avanto scanner. At 3.0-T, a readout segmented EPI (rs-EPI) sequence was performed with the following parameters: TR/TE, 8880/69 ms; flip angle, 180°; FOV, 340×207 mm; acquisition matrix, 256×156; slice thickness, 3 mm; acquisition time, 7 min 42 sec; spatial resolution, 1.3×1.3×3 mm; and b-values of 0, 800, and 1200 sec/mm$^2$ on a Siemens Skyra scanner. At 3.0-T, an ss-EPI sequence was performed with the following parameters: TR/TE/inversion time [TI], 9451/74/230 ms; FOV, 340×212 mm; acquisition

matrix, 256×160; reconstruction matrix, 320×200; slice thickness, 3 mm; acquisition time, 6:46; spatial resolution, 1.1×1.1×3 mm; and b-values of 0, 800, and 1200 sec/mm$^2$ on a Philips Ingenia scanner. An ADC value was calculated based on b=0 and 800 sec/mm$^2$ DW MRI scans.

### 2.3. Image analysis

Two breast radiologists (A.R.P and H.H.K., with 2 and 27 years of experience in breast imaging, respectively) retrospectively reviewed all MRI scans to reach a consensus. All T1-weighted images were transferred to a computer-aided detection (CAD) system (CADstream®, version 6.0.1; Confirma, WA). We used the CAD-generated tumor maximum diameter as the tumor size. The percent decrease in size was calculated as follows: Size decrease (%) = [($size_{post}$ - $size_{pre}$)/$size_{pre}$] x 100, where $size_{pre}$ and $size_{post}$ represent the pre- and posttreatment tumor size on MRI1 and MRI2, respectively.

ADC maps were automatically calculated and ADC values were derived on a voxel-by-voxel bases according to the following equation: ADC = - ln [S1/S0]/ (b1-b0), where S0 and S1 are signal intensities in the region of interest (ROI) obtained by two gradient factors, $b_0$ and $b_1$, respectively ($b_0$=0 sec/mm$^2$ and $b_1$=800 sec/mm$^2$). The tumor ROIs were drawn using a semi-automatic segmenting tool in Image J (National Institutes of Health, Bethesda, MD. USA) to measure the 3-dimensional mean ADC values encompassing the whole tumor. DCE MRI and T2-weighted images were used to guide positioning of the ROI within the solid part of the tumor, avoiding cystic and necrotic areas. When two or more lesions were present, we only selected the index lesion with the largest diameter for the study. When the tumor was assessed as being in complete remission on MRI2, the tumor ROI was drawn at the site of the previous lesion by referring to MRI1. The ΔADC was calculated as follows: ΔADC = $ADC_{post}$ - $ADC_{pre}$, where $ADC_{pre}$ and $ADC_{post}$ represent the pre- and posttreatment ADC values measured on MRI1 and MRI2, respectively.

### 2.4. Histopathologic analysis

All patients in this study were diagnosed with breast cancer by means of a core needle biopsy. Tumor features were obtained from the histopathologic reports of the biopsies performed before NAC. Tumors were categorized as one of the following subtypes based on immunohistochemistry results: luminal A (ER- and/or PR-positive, Ki-67 < 20%, and HER2-negative); luminal B (ER- and/or PR-

positive with either Ki-67 ≥ 20% or HER2-positive); HER2-enriched (ER/PR-negative and HER2-positive); and triple-negative (ER/PR-negative and HER2-negative).

Treatment response was determined by histopathologic examinations of the surgical specimens obtained after NAC. Pathological tumor responses were defined as either a complete pathologic response (pCR) [absence of residual invasive cancer cells in the breast and axilla (ypT0 and pN0)] or an incomplete response (non-pCR) [residual invasive disease observed in the breast and axilla]. Pathological tumor responses were evaluated according to the Miller-Payne grading system, which compares the cancer cellularity of the biopsy before NAC with that of the resected tumor after NAC. In the Miller-Payne grading system, grade 5 indicates pCR, and the remaining grades 1, 2, 3, and 4 indicate a partial pathological response .

### 2.5. Statistical analysis

SPSS for Windows (version 23, IBM) was used for statistical analysis. To compare the baseline patient characteristics between the pCR and non-pCR groups, the *t*-test or Mann-Whitney test for continuous variables and the Chi-square test for categorical variables were used. Factors associated with the prediction of pCR were assessed among the baseline patient characteristics by using multivariable logistic regression analysis with backward elimination. The predictive value of ΔADC for pCR was analyzed with an interaction effect between ΔADC and tumor subtype in the multivariate model. Receiver operating characteristic (ROC) curves were constructed to assess the diagnostic performance of ΔADC for pCR prediction, and the area under the curve (AUC) and 95% confidence intervals (CIs) were calculated. The optimal threshold was obtained based on the Youden index on the ROC curve. $P < 0.05$ was indicative of statistical significance.

# 3. Results

## 3.1. Patients

1,554 consecutive women with breast cancer who underwent breast MRI scans before and after NAC were identified. Women who had vacuum-assisted or excisional biopsy before the pretreatment MRI (n= 127), either pretreatment or posttreatment MRI performed at an outside institution or missing (n= 441), MRI scans insufficient for analysis (n= 272), or incomplete patient data (n= 280) were excluded. This study ultimately included a total of 434 women with breast cancer (mean age, 49 years; range, 41-58 years) (Figure 1).

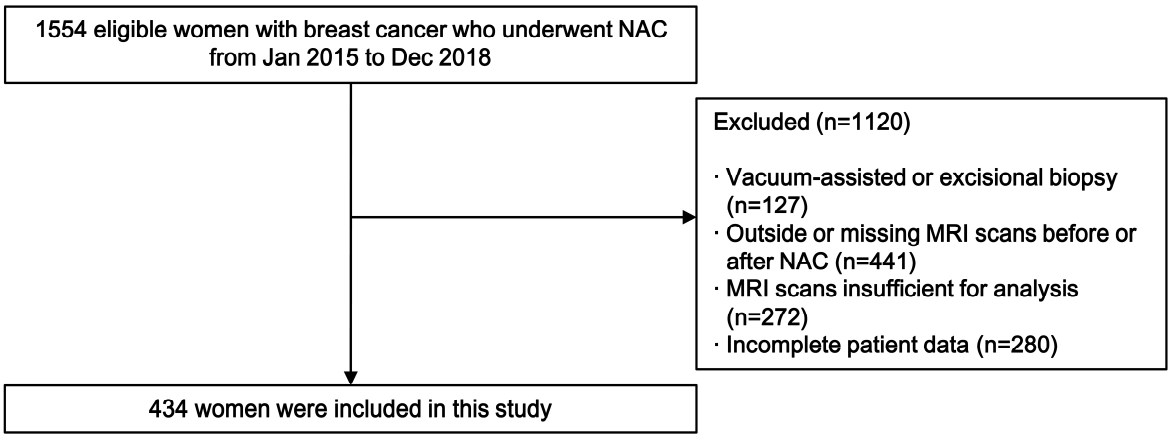


**Figure 1.** Flowchart of the study population in this study

Of the total 434 women, 103 (23.7%) achieved pCR and 331 (76.3%) did not. There was no significant difference in the mean age between the pCR and non-pCR groups. **Table 1** shows the baseline characteristics of the study population. In terms of the histopathologic analysis, 421 (97.0%) cases were diagnosed as invasive ductal carcinoma, 4 (0.9%) as invasive lobular carcinoma, and 9 (2.1%) as other histologic types (4 metaplastic carcinomas, 2 invasive mammary carcinomas, and 3 invasive carcinomas with a signet ring cell component or neuroendocrine and mesenchymal differentiation). There was no significant difference in the patient ages, histologic types, and histologic grades between the two groups. However, the nuclear grade, ER, PR, and HER2 status, Ki-67 positivity, and tumor subtypes were significantly different between the two groups.

**Table 1. Summary of the baseline characteristics of the study population**

| Characteristics | | Total (N= 434) | pCR group (N = 103) | non-pCR group (N = 331) | *P* Value |
|---|---|---|---|---|---|
| Age (years)* | | 49 ± 9 | 50 ± 9 | 49 ± 8 | 0.22 |
| Histologic type | IDC | 421 (97) | 101 (98) | 320 (97) | 0.69 |
| | ILC | 4 (0.9) | 1 (1.0) | 3 (0.9) | |
| | Others | 9 (2.1) | 1 (1.0) | 8 (2.4) | |
| Histologic grade | Low (grade 1, 2) | 298 (69) | 60 (58) | 238 (72) | 0.55 |
| | High (grade 3) | 136 (31) | 43 (42) | 93 (28) | |
| Nuclear grade | Low (grade 1, 2) | 294 (68) | 60 (58) | 234 (71) | 0.02† |
| | High (grade 3) | 14 (32) | 43 (42) | 97 (29) | |
| Estrogen receptor | Negative | 185 (43) | 71 (69) | 114 (34) | 0<0.001† |
| | Positive | 249 (57) | 32 (31) | 217 (66) | |
| Progesterone receptor | Negative | 254 (59) | 96 (93) | 158 (48) | 0<0.001† |

| | | | | | |
|---|---|---|---|---|---|
| | Positive | 180 (42) | 7 (6.8) | 173 (52) | |
| HER2 | Negative | 290 (67) | 36 (35) | 254 (77) | 0<0.001† |
| | Positive | 144 (33) | 67 (65) | 77 (23) | |
| Ki-67 | Low (<20%) | 47 (11) | 2 (1.9) | 45 (14) | 0.01† |
| | High (≥20%) | 387 (89) | 101 (98) | 286 (86) | |
| Tumor subtype | Luminal A | 43 (9.9) | 1 (1.0) | 42 (13) | 0<0.001† |
| | Luminal B | 207 (48) | 31 (30) | 176 (53) | |
| | HER2-enriched | 76 (18) | 44 (43) | 32 (9.7) | |
| | Triple-negative | 108 (25) | 27 (26) | 81 (25) | |

Note.– Except where indicated, data are numbers of patients, and data in parentheses are percentages.

* Data are reported as the mean ± standard deviation.

† Statistically significant.

IDC = invasive ductal carcinoma, ILC = invasive lobular carcinoma, HER2 = human epidermal growth factor receptor 2

### 3.2. Tumor response and comparison of MRI parameters

**Table 2** shows the MRI parameters including the tumor size and mean ADC values from MRI scans obtained before and after NAC. There was no difference in the maximum tumor diameter on MRI1 between the pCR and non-pCR groups (3.7±1.8 vs. 3.9±1.6, *P*=0.27). However, the maximum tumor diameter on MRI2 was significantly smaller and the percentage decrease in size was greater in the pCR group than in the non-pCR group (0.2±0.7 vs. 2.2±1.8 and 95.4±14.3 vs. 45.4±34.2, respectively, *P*<0.001). In terms of the mean ADC values ($\times 10^{-3}$ $mm^2/s$), the ADC on MRI1 was not significantly different between the two groups (0.9±0.3 vs. 0.9±0.3, *P*=0.63). However, the ADC on MRI2 was significantly higher in the pCR group than in the non-pCR group (1.5±0.5 vs. 1.2±0.4, *P*<0.001), and ΔADC was significantly greater in the pCR group than in the non-pCR group (0.5±0.6 vs. 0.2±0.4 *P*<0.001). Examples of the DW MRI and ADC values in the study patients in the pCR and non-pCR groups are shown in **Figures 2 and 3**, respectively.

**Table 2. Comparison of MRI parameters including tumor size and ADC values between the pCR and non-pCR groups**

| MRI parameters | pCR group (N = 103) | non-pCR group (N = 331) | *P* value |
|---|---|---|---|
| Maximum tumor diameter on MRI1 (mm) | 3.7 ± 1.8 | 3.9 ± 1.6 | 0.27 |
| Maximum tumor diameter on MRI2 (mm) | 0.2 ± 0.7 | 2.2 ± 1.8 | 0<0.001† |
| Size decrease (%) | 95 ± 14 | 45 ± 34 | 0<0.001† |
| ADC on MRI1 ($\times 10^{-3}$ $mm^2/s$) | 0.9 ± 0.3 | 0.9 ± 0.3 | 0.63 |
| ADC on MRI2 ($\times 10^{-3}$ $mm^2/s$) | 1.5 ± 0.5 | 1.2 ± 0.4 | 0<0.001† |
| ΔADC ($\times 10^{-3}$ $mm^2/s$) | 0.5 ± 0.6 | 0.2 ± 0.4 | 0<0.001† |

Note.– Data are reported as the mean ± standard deviation.

† Statistically significant.

MRI1 = MRI exam prior to NAC, MRI2: MRI exam after completion of NAC, ADC= apparent diffusion coefficient.

$\Delta ADC = [ADC_{post} - ADC_{pre}]$, where $ADC_{pre}$ and $ADC_{post}$ represent pre- and posttreatment ADC values measured on pre- and posttreatment MRI exams, respectively.

a b c d

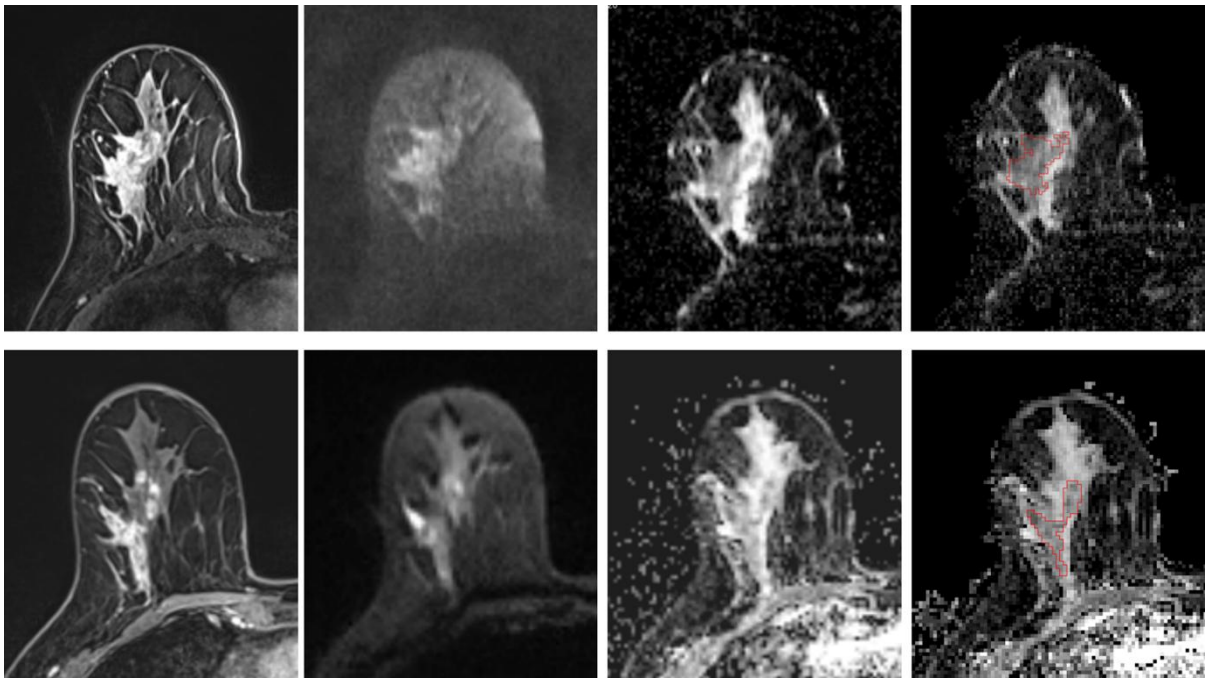

**Figure 2.** Images of a 55 year-old woman who underwent NAC for invasive ductal carcinoma with the human epidermal growth factor receptor 2-enriched subtype in the right breast and who achieved a pathologic complete response after 6 cycles of NAC. Axial post-contrast T1-weighted MRI images (a), DW MRI images (b=800 sec/mm$^2$) (b), and ADC maps (c, d) are shown. With reference to the DCE MRI scans (a), a whole-tumor region of interest (ROI) was defined across multiple sections of each DW MRI scan, and the mean ADC was calculated for all voxels in the ROI. Before NAC (in the first row), the lesion was visualized as an approximately 8.5-cm segmentally distributed clumped nonmass enhancement lesion extending to subareolar area on the DCE MRI scan (a, in the first row). The mean ADC value was 1.0 sec/mm$^2$ (d, in the first row). After NAC (in the second row), the maximum tumor diameter was approximately 4.7 cm on the DCE MRI scan (a, in the second row), and the mean ADC value was 1.4 sec/mm$^2$ (d, in the second row). NAC = neoadjuvant chemotherapy, DW MRI = diffusion-weighted MRI, ADC = apparent diffusion coefficient, DCE MRI = dynamic contrast-enhanced MRI.

a b c d

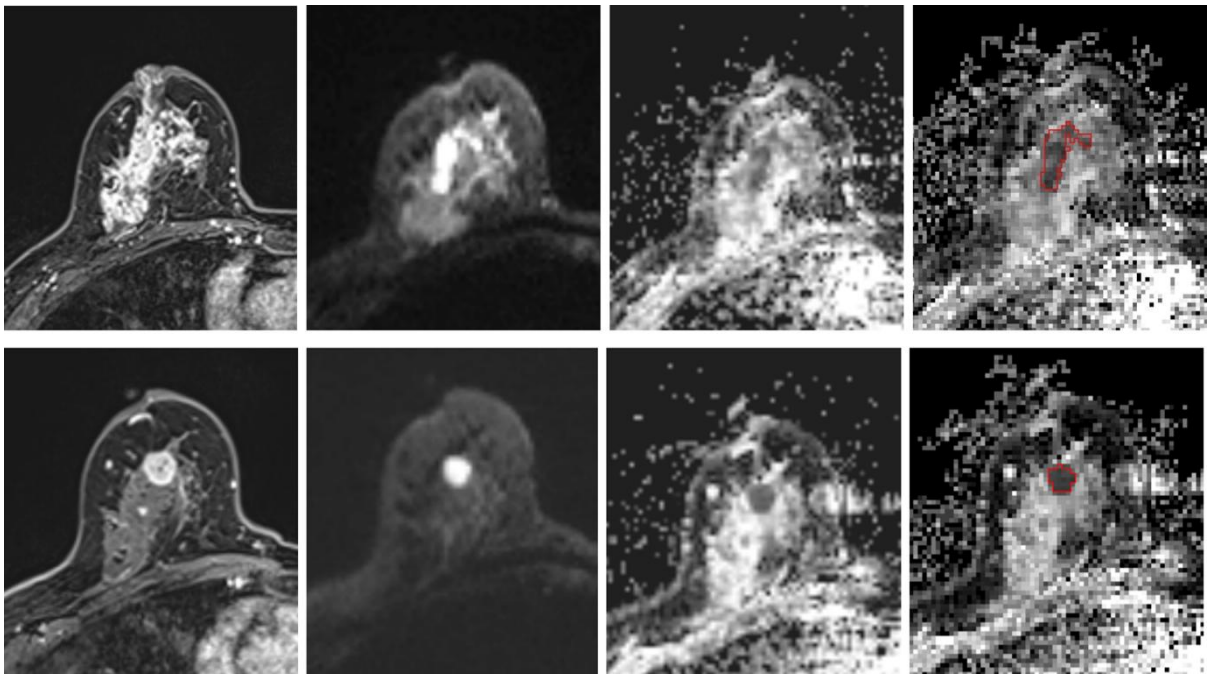

**Figure 3.** Images of a 56 year-old woman who underwent NAC for invasive ductal carcinoma with the luminal B subtype (estrogen receptor-positive, progesterone receptor-negative, and HER2-positive) in the right breast who did not achieve a pathologic complete response after 6 cycles of NAC. Axial post-contrast T1-weighted MRI images (a), DW MRI images (b=800 sec /mm$^2$) (b), and ADC maps (c, d) are shown. With reference to the DCE MRI scans (a), a whole-tumor region of interest (ROI) was defined across multiple sections of each DW MRI scan, and the mean ADC was calculated for all voxels in the ROI. Before NAC (in the first row), the lesion was visualized as an approximately 6.5-cm enhancing mass and nonmass lesion extending to the subareolar area with nipple retraction on the DCE MRI scan (a, in the first row). The mean ADC value was 1.3 sec/mm$^2$ (d, in the first row). After NAC (in the second row), the maximum tumor diameter was approximately 2.3 cm on the DCE MRI scan (a, in the second row), and the mean ADC value was 0.8 sec/mm$^2$ (d, in the second row). NAC = neoadjuvant chemotherapy, DW MRI = diffusion-weighted MRI, ADC = apparent diffusion coefficient, DCE MRI = dynamic contrast-enhanced MRI.

### 3.3. Effect of tumor subtype

Treatment response varies in accordance with underlying tumor characteristics. In this study, according to the tumor subtype, the HER2-enriched subtype showed the highest pCR rate (58%), followed by triple-negative (25%), luminal B (15%), and luminal A (2%) subtypes. The distributions of ΔADC in the pCR and non-pCR groups according to tumor subtype are shown in **Figure 4.** We explored the potential effect of the interaction between the tumor subtype and ΔADC in predicting pCR and then investigated the predictive value of ΔADC for pCR (**Table 3**). The multivariate analysis model included covariates including size decrease (%), PR status, and HER2 status that were selected by a backward elimination method. In the multivariate analysis before adjustment for tumor subtype, ΔADC was not found to be an independent predictor of pCR ($P$=0.48, data not shown). However, a significant interaction was found between the tumor subtype and ΔADC for the prediction of pCR ($P$ for interaction=0.02) in the entire cohort. Furthermore, among the tumor subtypes, ΔADC was significantly associated with pCR in only the HER2-enriched subtype (adjusted odds ratio=5.70, 95% CI: 1.25, 32.70, $P$=0.04) in the multivariate analysis including an interaction effect.

In the ROC curve analysis, the optimal cut-off value of ΔADC to distinguish between pCR and non-pCR was 0.55 (95% CI: 0.58, 0.72, $P$<0.001) in the entire study population, yielding 52.4% sensitivity and 80.7% specificity, and the AUC was 0.65 (**Figure 5a**). In the HER2-enriched subtype, the optimal cut-off value of ΔADC for predicting pCR was 0.21, yielding a sensitivity of 81.8% and a specificity of 71.9%, and the AUC was 0.77 (95% CI: 0.65, 0.88, $P$<0.001) (**Figure 5b**).

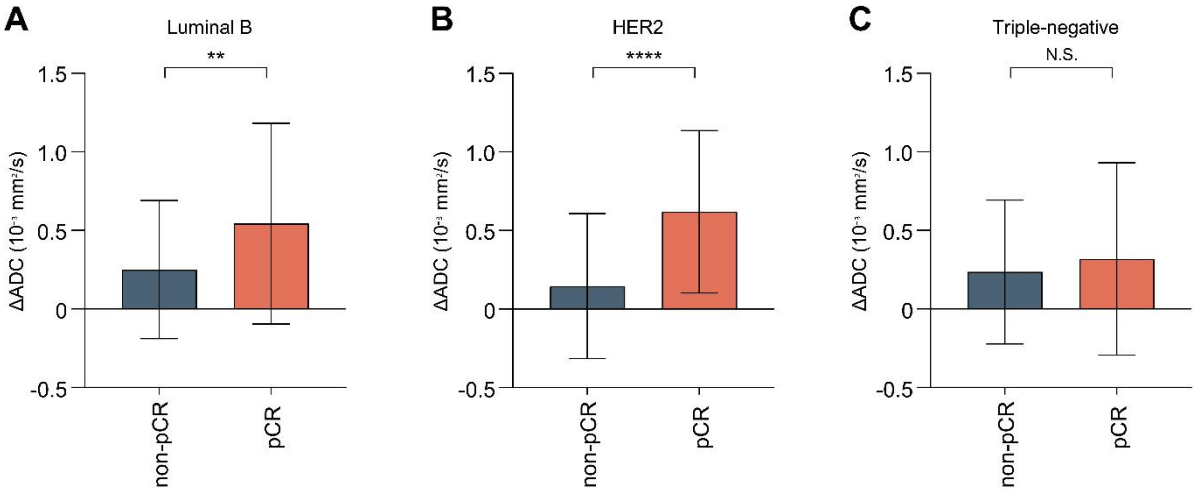


**Figure 4.** Distributions of ΔADC in the pCR and non-pCR groups according to the tumor subtype including luminal B (A), HER2-enrhiced (B), and triple-negative (C) subtypes. Each box plot shows the mean difference in the ADC value (ΔADC) and standard deviations as the height of the box and the two horizontal lines above and below the boxes, respectively, in the non-pCR and pCR groups.

** indicates a *P* value less than 0.05, and *** indicates a *P* value less than 0.001. N.S. indicates a nonsignificant *P* value.

**Table 3. Predictive value of ΔADC for pCR with an interaction effect for tumor subtype**

| Effect | Tumor subtype | Crude | | | Adjusted* | | |
|---|---|---|---|---|---|---|---|
| | | Odds ratio | 95% CI | *P* value | Odds ratio | 95% CI | *P* value |
| ΔADC | Total | | | 0.07** | | | 0.02**† |
| | Luminal A | 0.10 | 0.00–27.30 | 0.40 | 0.01 | 0.00–5.40 | 0.14 |
| | Luminal B | 3.48 | 1.57–7.97 | 0.002† | 1.80 | 0.61–5.89 | 0.30 |
| | HER2-enriched | 7.47 | 2.62–26.00 | <0.001† | 5.70 | 1.25–32.70 | 0.04† |
| | Triple-negative | 1.40 | 0.58–3.44 | 0.46 | 0.43 | 0.14–1.27 | 0.13 |

* This multivariate analysis model included the size percent decrease, PR status, and HER2 status as covariates that were selected by a backward elimination method. Variables with a $P < 0.1$ in the univariate analysis were included in the multivariate analysis.

**$P$ value for interaction.

† Statistically significant.

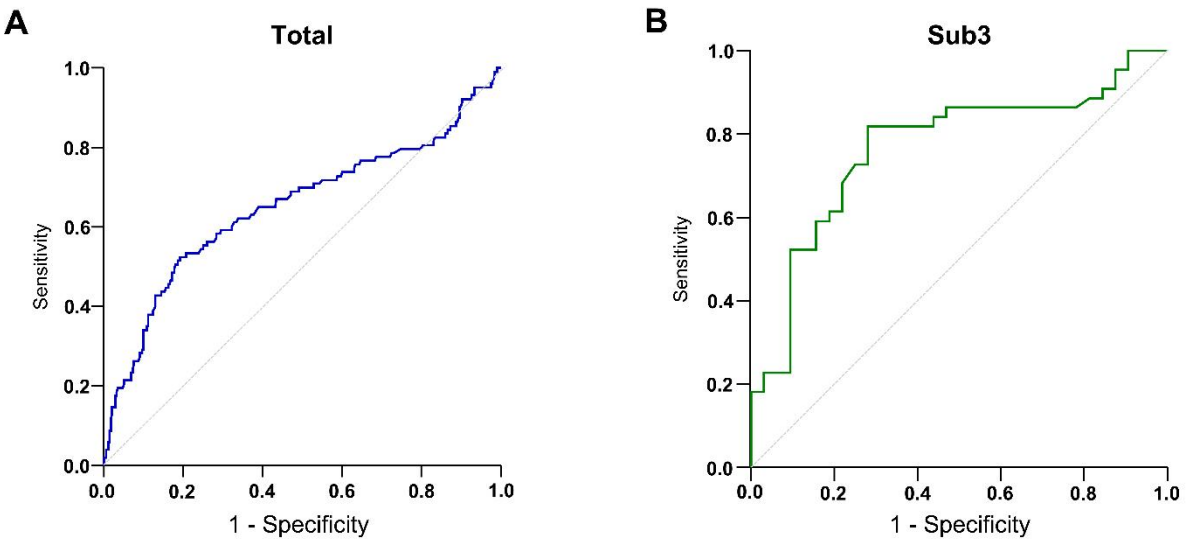


**Figure 5.** ROC curves to evaluate ΔADC as a predictor of pCR in the entire study population (A) and the HER2-enriched tumor subtype group (B).

# 4. DISCUSSION

In this study, we evaluated the utility of DWI for predicting pathological response to NAC in patients with breast cancer. We found that the increase in mean tumor ADC value was greater in the pCR group than in the non-pCR group (0.5±0.6 vs. 0.2±0.4, $P$<0.001). There was also a significant interaction between the tumor subtype and ΔADC for predicting pCR ($P$ for interaction=0.02) in the entire cohort. According to the tumor subtype, ΔADC was found to be an independent predictor of pCR in only the HER2-enriched subtype (adjusted odds ratio=5.70, 95% CI: 1.25, 32.70, $P$=0.04). To our knowledge, there has been limited studies to assess the usability of the tumor ADC as a predictor of pCR while including an interaction effect between the tumor subtype and ADC.

Many studies have investigated the use of ADC to predict pCR . The ACRIN 6698 trial , a prospective multicenter study, revealed that ΔADC mid- and posttreatment was significantly different between the pCR group and the counterpart, as shown in our study. In the study by Shin et al , the percentage change in ADC was significantly higher in the pCR group than in the non-pCR group. Several studies have investigated the role of ADC for early prediction of pCR during NAC. Regarding the role of the pretreatment ADC, there has been inconsistent results . In our study, the pretreatment ADC was not significantly different between the two groups. However, the posttreatment ADC was significantly different between the pCR and non-pCR groups, as shown in previous studies .

As breast cancer is a heterogeneous disease, the pathological response to NAC differs between the tumor subtypes . In this study, ΔADC was predictive of pCR in only the HER2-enriched subtype with the AUC of 0.77 (95% CI: 0.65, 0.88, $P$<0.001). However, only a few studies have evaluated the predictive value of the ADC for pCR considering the effect of the tumor subtype. There is also a lack of consistency in the definition for pCR. In the study by Liu et al , after comparison between two subtypes, the post-NAC ADC value of the triple-negative subtype was significantly higher than those of the other three subtypes ($P$<0.001) and that of HER2-enriched subtype was significantly higher than luminal A ($P$<0.001) and luminal B subtypes ($P$=0.001). However, they included grade 4 as well as grade 5 lesions of the Miller-Payne grading system for pCR, and metastatic axillary lymph node status was not considered in the study. Moreover, they excluded patients who had received a trastuzumab-based regimen. In the ACRIN 6698 trial , percentage change in ADC posttreatment was found to be predictive of pCR in only the triple-negative subtype ($P$<0.001). However, the proportion of the study population was imbalanced in their study, with relatively higher portion of the triple-negative subtype (77/242, 32%, second most followed after the luminal A (99/242). Also, their subgroup analysis results

could have been affected by the study cohort that excluded patients with low-risk hormone receptor-positive and HER2-negative disease.

Regarding assessment of the tumor ADC value, the definition of an ROI on the ADC map has not been uniform among the studies. Previous studies have mentioned the limitations of manual drawing of tumor ROIs. Belli et al demonstrated that the single ROI method had superior diagnostic accuracy to the multiple ROI method. However, according to the recent guideline from the European Society of Breast Radiology (EUSOBI) International Breast DWI working group , volumetric sampling of the whole lesion might be useful in case of evaluating the tumor response. In our study, the 3-dimensional ADC value of the ROI across the entire lesion was obtained using software.

There are limitations in this study. First, this was a retrospective study conducted at a single institution. Second, the patient population in each tumor subtype was not evenly distributed. It was particularly observed in luminal A subtype, which had only one patient among those who achieved pCR.

In conclusion, we investigated the role of ΔADC to predict pCR in patients with breast cancer undergoing NAC before surgery. Our data suggest that an increase in the tumor ADC value after NAC is an independent predictor of pCR in the HER2-enriched subtype. Notably, this is the first study to use an interaction effect in the analysis of DWI for prediction of pCR, and we defined the tumor ROIs semi-automatically to enhance the reproducibility and accuracy. Further prospective studies with a sufficient number of patients for each tumor subtype are required to verify the use of ΔADC for pCR prediction.

## References


1. Fisher B, Brown A, Mamounas E et al (1997) Effect of preoperative chemotherapy on local-regional disease in women with operable breast cancer: findings from national surgical adjuvant breast and bowel project B-18. J Clin Oncol 15:2483-2493

2. Rastogi P, Anderson SJ, Bear HD et al (2008) Preoperative chemotherapy: updates of national surgical adjuvant breast and bowel project protocols B-18 and B-27. J Clin Oncol 26:778-785

3. van der Hage JA, van de Velde CJ, Julien JP, Tubiana-Hulin M, Vandervelden C, Duchateau L (2001) Preoperative chemotherapy in primary operable breast cancer: results from the European organization for research and treatment of cancer trial 10902. J Clin Oncol 19:4224-4237

4. Cortazar P, Zhang L, Untch M et al (2014) Pathological complete response and long-term clinical benefit in breast cancer: the CTNeoBC pooled analysis. Lancet 384:164-172

5. Yeh E, Slanetz P, Kopans DB et al (2005) Prospective comparison of mammography, sonography, and MRI in patients undergoing neoadjuvant chemotherapy for palpable breast cancer. AJR Am J Roentgenol 184:868-877

6. von Minckwitz G, Untch M, Blohmer JU et al (2012) Definition and impact of pathologic complete response on prognosis after neoadjuvant chemotherapy in various intrinsic breast cancer subtypes. J Clin Oncol 30:1796-1804

7. Woodhams R, Ramadan S, Stanwell P et al (2011) Diffusion-weighted imaging of the breast: principles and clinical applications. Radiographics 31:1059-1084

8. Partridge SC, Zhang Z, Newitt DC et al (2018) Diffusion-weighted MRI findings predict pathologic response in neoadjuvant treatment of breast cancer: the ACRIN 6698 multicenter trial. Radiology 289:618-627

9. Partridge SC, Gibbs JE, Lu Y, Esserman LJ, Sudilovsky D, Hylton NM (2002) Accuracy of MR imaging for revealing residual breast cancer in patients who have undergone neoadjuvant chemotherapy. AJR Am J Roentgenol 179:1193-1199

10. Kim H, Kim HH, Park JS et al (2014) Prediction of pathological complete response of breast cancer patients undergoing neoadjuvant chemotherapy: usefulness of breast MRI computer-aided detection. Br J Radiol 87:20140142

11. Gu YL, Pan SM, Ren J, Yang ZX, Jiang GQ (2017) Role of magnetic resonance imaging in detection of pathologic complete remission in breast cancer patients treated with neoadjuvant chemotherapy: a meta-analysis. Clin Breast Cancer 17:245-255

12. Belli P, Costantini M, Ierardi C et al (2011) Diffusion-weighted imaging in evaluating the response to neoadjuvant breast cancer treatment. Breast J 17:610-619

13. Fangberget A, Nilsen LB, Hole KH et al (2011) Neoadjuvant chemotherapy in breast cancer-response evaluation and prediction of response to treatment using dynamic contrast-enhanced and diffusion-weighted MR imaging. Eur Radiol 21:1188-1199

14. Park SH, Moon WK, Cho N et al (2010) Diffusion-weighted MR imaging: pretreatment prediction of response to neoadjuvant chemotherapy in patients with breast cancer. Radiology 257:56-63

15. Shin HJ, Baek HM, Ahn JH et al (2012) Prediction of pathologic response to neoadjuvant chemotherapy in patients with breast cancer using diffusion-weighted imaging and MRS. NMR Biomed 25:1349-1359

16. Richard R, Thomassin I, Chapellier M et al (2013) Diffusion-weighted MRI in pretreatment prediction of response to neoadjuvant chemotherapy in patients with breast cancer. Eur Radiol 23:2420-2431

17. Pereira NP, Curi C, Osorio C et al (2019) Diffusion-weighted magnetic resonance imaging of patients with breast cancer following neoadjuvant chemotherapy provides early prediction of pathological response: a prospective study. Sci Rep 9:16372

18. Liu S, Ren R, Chen Z et al (2015) Diffusion-weighted imaging in assessing pathological response of tumor in breast cancer subtype to neoadjuvant chemotherapy. J Magn Reson Imaging 42:779-787

19. Kaufmann M, von Minckwitz G, Mamounas EP et al (2012) Recommendations from an international consensus conference on the current status and future of neoadjuvant systemic therapy in primary breast cancer. Ann Surg Oncol 19:1508-1516

20. Kim MM, Allen P, Gonzalez-Angulo AM et al (2013) Pathologic complete response to neoadjuvant chemotherapy with trastuzumab predicts for improved survival in women with HER2-overexpressing breast cancer. Ann Oncol 24:1999-2004

21. Ogston KN, Miller ID, Payne S et al (2003) A new histological grading system to assess response of breast cancers to primary chemotherapy: prognostic significance and survival. Breast 12:320-327

22. Santamaria G, Bargallo X, Fernandez PL, Farrus B, Caparros X, Velasco M (2017) Neoadjuvant systemic therapy in breast cancer: association of contrast-enhanced MR imaging findings, diffusion-weighted imaging findings, and tumor subtype with tumor response. Radiology 283:663-672

23. Ramirez-Galvan YA, Cardona-Huerta S, Elizondo-Riojas G, Alvarez-Villalobos NA (2018) Apparent diffusion coefficient value to evaluate tumor response after neoadjuvant chemotherapy in patients with breast cancer. Acad Radiol 25:179-187

24. Jensen LR, Garzon B, Heldahl MG, Bathen TF, Lundgren S, Gribbestad IS (2011) Diffusion-weighted and dynamic contrast-enhanced MRI in evaluation of early treatment effects during neoadjuvant chemotherapy in breast cancer patients. J Magn Reson Imaging 34:1099-1109

25. Sharma U, Danishad KK, Seenu V, Jagannathan NR (2009) Longitudinal study of the assessment by MRI and diffusion-weighted imaging of tumor response in patients with locally advanced breast cancer undergoing neoadjuvant chemotherapy. NMR Biomed 22:104-113

26. Hu XY, Li Y, Jin GQ, Lai SL, Huang XY, Su DK (2017) Diffusion-weighted MR imaging in prediction of response to neoadjuvant chemotherapy in patients with breast cancer. Oncotarget 8:79642-79649

27. Bhargava R, Beriwal S, Dabbs DJ et al (2010) Immunohistochemical surrogate markers of breast cancer molecular classes predicts response to neoadjuvant chemotherapy: a single institutional experience with 359 cases. Cancer 116:1431-1439

28. Goldhirsch A, Wood WC, Coates AS et al (2011) Strategies for subtypes--dealing with the diversity of breast cancer: highlights of the St. Gallen international expert consensus on the primary therapy of early breast cancer 2011. Ann Oncol 22:1736-1747

29. Baltzer P, Mann RM, Iima M et al (2020) Diffusion-weighted imaging of the breast-a consensus and mission statement from the EUSOBI international breast diffusion-weighted imaging working group. Eur Radiol 30:1436-1450

30. Januskeviciene I, Petrikaite V (2019) Heterogeneity of breast cancer: The importance of interaction between different tumor cell populations. Life Sci 239:117009

31. Bianchini G, Balko JM, Mayer IA, Sanders ME, Gianni L (2016) Triple-negative breast cancer: challenges and opportunities of a heterogeneous disease. Nat Rev Clin Oncol 13:674-690

## Abstract

Apparent diffusion coefficient (ADC) on diffusion-weighted imaging (DWI) has a potential role to predict pathological response in patients with breast cancer undergoing neoadjuvant chemotherapy (NAC). The response to NAC varies according to the molecular subtype of breast cancer. However, only a few studies have demonstrated the usefulness of the ADC as a predictor of pathological complete response (pCR) while considering the effect of the tumor subtype. Therefore, I investigated the efficacy of ADC for predicting pCR in patients with breast cancer after NAC, including an interaction between ADC and the tumor subtype.

Women with breast cancer who underwent breast MRI before and after completion of NAC before surgery between 2015 and 2018 were retrospectively identified. Mean ADC values of the tumor on pre- and post-NAC DWI ($ADC_{pre}$ and $ADC_{post}$, respectively) were measured. The change in the mean tumor ADC value (ΔADC) was calculated as follows: $\Delta ADC = ADC_{post} - ADC_{pre}$. The pathological response was classified into either a complete response (pCR) or an incomplete response (non-pCR) according to the Miller & Payne grading system. The predictive value of ADC for pCR was assessed including the interaction of the tumor subtype.

Among 434 women, 103 (23.7%) achieved pCR (pCR group), and 331 (76.3%) did not (non-pCR group). $ADC_{post}$ and ΔADC values were significantly different between the pCR and non-pCR groups (1.5±0.5 vs. 1.2±0.4 and 0.5±0.6 vs. 0.2±0.4, respectively; $P<0.001$). A significant interaction was found between the tumor subtype and ΔADC for predicting pCR ($P$ for interaction=0.02) in the entire cohort. Among the tumor subtypes, ΔADC was significantly associated with pCR in only the HER2-enriched subtype (adjusted odds ratio= 5.70, $P=0.04$). In receiver operating characteristic curve analysis, the area under the curve (AUC) was 0.65 in entire cohort, and the AUC was 0.77 in patients with the HER2-enriched subtype.

In conclusion, the results indicate that an increase in the mean tumor ADC value on DWI after NAC is useful for predicting pCR. The ΔADC was an independent predictive factor for pCR in only patients with the HER2-enriched subtype.



Keywords: Breast cancer; Apparent diffusion coefficient (ADC); Diffusion-weighted imaging (DWI); Magnetic Resonance Imaging (MRI); Neoadjuvant chemotherapy; Pathological response; Tumor subtype